ELSEVIER

Journal of Alloys and Compounds 351 (2003) 158–170

Journal of ALLOYS AND COMPOUNDS

www.elsevier.com/locate/jallcom

Thermodynamic assessment of the Cu–Ti–Zr system

R. Arroyave*, T.W. Eagar, L. Kaufman

DMSE, Massachusetts Institute of Technology, Cambridge, MA, USA

Received 13 June 2002; received in revised form 9 September 2002; accepted 9 September 2002

Abstract

Equilibrium phase relations in the Cu–Ti–Zr system are calculated using the Calphad approach. Thermodynamic model parameters for the Ti–Zr, Cu–Ti and Cu–Zr systems, previously obtained in the literature, are used. New thermodynamic descriptions for the ternary interaction parameters of the liquid are obtained from experimental information. Additionally, the Gibbs energy of formation for the ternary phase Cu_2TiZr phase is also assessed from experimental data. A new description of the $CuTi_2$ and $CuZr_2$ phases, treated as single phases, is developed. The parameters obtained in this assessment are later used for the calculation of selected isothermal sections and the projected liquidus surface of this system over the entire composition range. This model allows the prediction of a series of invariant points involving the liquid phase, at lower temperatures than neighboring binary eutectics.

Keywords: Transition metal alloys; Phase diagram; Liquid alloys; Thermodynamic modelling

1. Introduction

The Cu–Ti and Cu–Zr systems are characterized by the presence of a series of invariant points involving the liquid phase and a series of solid solutions and inter-metallic compounds (see Fig. 1, after [1] and Fig. 2, after [2]). In both systems, the enthalpy of mixing of the corresponding liquid solutions is highly exothermic [3] and thus contributes to the large stability of the liquid phase with respect to the different crystalline phases. This large relative stability promotes the existence of eutectic and peritectic points at much lower temperatures (ΔT~400–~600 °C) than the melting point of the pure components.

If a relatively stable liquid phase—which can be inferred by the presence of deep eutectics at temperatures much lower than the melting temperatures of the pure components—with a composition sufficiently far away from the compositions of competing crystalline phases is rapidly quenched, the crystallization process can be frustrated and the formation of an amorphous phase is possible [4]. By using simple thermodynamic arguments, coupled with similarly simple kinetic concepts, it has been possible to predict the glass formation range (GFR) for a large number of binary alloy systems [4]. In general, this GFR correlates well with the regions of the phase diagram where the liquid is more stable than competing crystalline phases.

The Cu–Ti and Cu–Zr systems exhibit a wide GFR [5,6], which is consistent with the observed presence of a large number of eutectic points at temperatures much

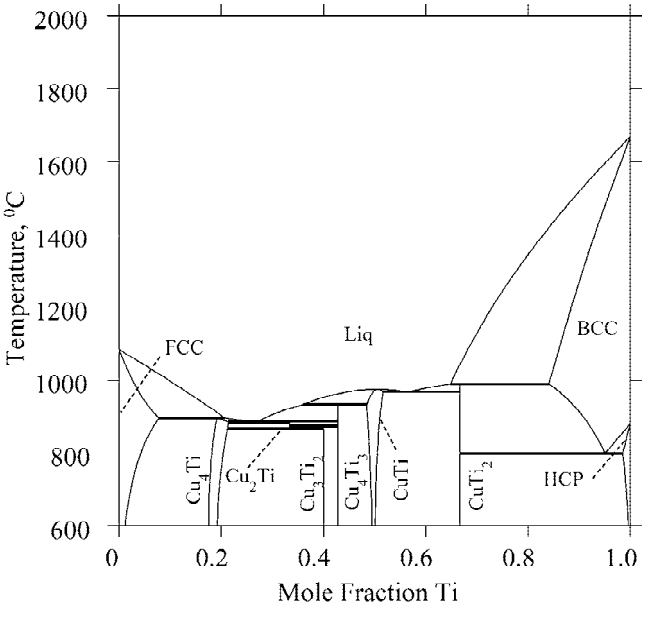

Fig. 1. Calculated Cu–Ti phase diagram, using thermodynamic assessment by Kumar et al. [1].

*Corresponding author.
E-mail address: raymundo@mit.edu (R. Arroyave).

0925-8388/02/$ – see front matter
PII: S0925-8388(02)01035-6

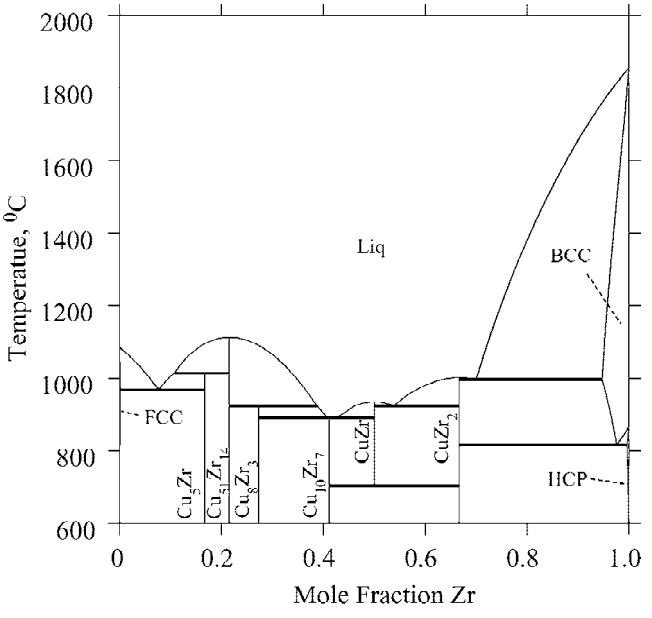

Fig. 2. Calculated Cu–Zr phase diagram, using thermodynamic assessment by Zeng et al. [2].

lower than the melting points of the pure components. It can then be expected that the corresponding ternary system, i.e. Cu–Ti–Zr would also exhibit a strong tendency for amorphous solidification. Although extensive experimental data regarding the GFR of ternary Cu–Ti–Zr alloys has been obtained (see [7]), the studies have been limited to rather narrow ranges of composition. Since experimental determination of the glass forming ability of Cu–Ti–Zr alloys over the entire compositional range is time-consuming and costly, a way of determining possible GFR from a theoretical point of view is extremely attractive. Once a rough search using adequate thermodynamic and kinetic criteria has been performed, it would then be easier to focus the experimental effort only on the most promising regions of system. Because of the increasing interest in the Cu–Ti–Zr system for amorphous alloy applications, it is important to develop a reliable thermodynamic model of the system that can be further used for calculation of the GFR.

For ternary and higher-order systems, a reliable thermodynamic model can be obtained using the information available from the lower order systems plus any ternary experimental data available. Thermodynamic parameters that describe binary interactions in the phases of interest can be used to extrapolate and calculate the thermodynamic properties of the higher-order systems [8]. In many cases, ternary interaction contributions to the total Gibbs energy of the phases can be neglected and the thermodynamic models for the binary systems can be used to obtain reliable predictions regarding the thermodynamic properties of the ternary over the entire compositional range, as well as the glass formation range of the system. This simple extrapolation cannot be done, however, when there are high-order phases (i.e. ternary compounds) present in the system. Trying to estimate the relative stability of the liquid phase in the central regions of the phase diagram without considering these ternary compounds could lead to overestimating the GFR for the ternary system.

Unfortunately, the ternary phase Cu_2TiZr has been detected in the Cu–Ti–Zr system [9,10]. Thus, a more realistic model accounting for ternary interactions for the liquid and other phases and a thermodynamic description of the Cu_2TiZr phase are needed to estimate the GFR of this system. In the present work, a self-consistent thermodynamic model for the Cu–Ti–Zr system was obtained using the CALPHAD approach [11]. Binary interaction parameters for the Cu–Ti, Cu–Zr and Ti–Zr systems were obtained from previous works [1,2,12] while ternary parameters for the *liquid* and *bcc* phases and new thermodynamic descriptions for the $Cu(Ti, Zr)_2$ (tetragonal $I4/mmm$, $MoSi_2$ type) solid solution and the ternary phase Cu_2TiZr were determined from experimental data using the least-squares minimization module PARROT [13] in the Thermo-Calc software package [14]. Using the resulting thermodynamic models, some isothermal ternary sections and the liquidus projection of the Cu–Ti–Zr system were calculated. Additionally, the compositions and temperatures of all the ternary invariant points involving the liquid phase were determined.

2. Experimental information

2.1. Phase relationships

Woychik et al. [9] studied the phase relation characteristics of the isothermal section of the Cu–Ti–Zr system at 703 °C. The great majority of the studied compositions corresponded to the Cu-rich region of the system. Microstructures of the resulting samples were analyzed using optical microscopy. The chemical composition of the samples was determined using electron microprobe analysis.

The phase relationships at 703 °C were determined by fitting of the corresponding three-phase triangles. However, it is not reported whether the different phases within the three-phase regions were identified using XRD or just by simple optical quantification. The authors report that both phases CuTi and Cu_3Ti_2 (more recent studies report the stoichiometry to be $Cu_{10}Zr_7$ [2]) present a certain degree of penetration into the ternary system, although there are only two data points corroborating this fact [9].

One of the dominant features of the 703 °C section was the presence of the ternary phase Cu_2TiZr. This phase greatly influences the shape of the liquidus at the central region of the phase diagram and is expected to be an important competing crystalline phase in amorphous solidification processing involving this system. It was also

observed that this phase enters into pseudo-binary equilibrium with most of the stable phases of the system at the experimental temperatures.

2.2. Investigation of eutectic reactions in the ternary system

To determine any possible eutectic reactions involving this phase, Woychik et al. [9] used the Transient Liquid Phase (TLP) bonding technique [15]. In this procedure, two phases, A and B, are brought into contact and assembled into a sandwich structure—*A*/*B*/*A*, for example—at a temperature higher than the invariant point involving these phases. If there were a eutectic reaction involving these two phases, inter-diffusion processes would eventually lead to the formation of a liquid layer at the *A*/*B* interfaces. A liquid thus formed gradually disappears as the inter-diffusion process continues. However, if the liquid is quenched before it disappears, the eutectic regions can be identified in the quenched microstructure and the composition of the liquid at the eutectic point can be determined. Woychik et al. [9] used diffusion couples involving Cu_2TiZr and either CuTi, CuZr or $CuZr_2$. The sandwich structures were held at temperatures around 867 °C for 30 min. From these experiments, the three eutectic reactions involving the Cu_2TiZr phase were determined:

$$\begin{aligned} &\mathrm{Liq} \rightarrow \mathrm{Cu_2TiZr} + \mathrm{CuZr} + \mathrm{CuZr_2} \\ &\mathrm{Liq} \rightarrow \mathrm{Cu_2TiZr} + bcc + \mathrm{CuZr_2} \\ &\mathrm{Liq} \rightarrow \mathrm{Cu_2TiZr} + \mathrm{CuTi} + \mathrm{CuTi_2} \end{aligned} \quad (1)$$

Using electron microprobe analysis, the eutectic compositions for the reactions given in Eq. (1) were obtained. Woychik et al. [9] reported the reactions in Eq. (1) based on optical verification of the number of phases present in the quenched liquid as well as its average composition (using electron micro-probe analysis). Although the authors mentioned the use of X-ray diffraction techniques in their analysis of the samples, no specific XRD phase identification procedure or results are reported.

2.3. $CuTi_2$–$CuZr_2$ pseudo-binary

Chebotnikov and Molokanov [10] studied the $CuTi_2$–$CuZr_2$ vertical region of the Cu–Ti–Zr system by preparing several alloys along the $x_{\mathrm{Ti}} + x_{\mathrm{Zr}} = 2/3$ iso-compositional line. For each composition, a sample was annealed at 697 °C for 200 h and later quenched in water. XRD analyses were performed both at high (297–697 °C) and room temperatures. Furthermore, DTA analysis was done on each of the samples for the entire temperature range until complete melting was detected.

XRD analyses showed that the alloys had linearly increasing *a* and *c* unit-cell parameters—while the ratio *c*/*a* decreased—as the amount of Zr increased over the entire compositional range. This indicated that the alloys formed a single phase in which Zr and Ti atoms could be exchanged within the same lattice site of the unit cell. In these XRD analyses, small amounts of a ternary phase (of unreported composition) in the central region of this iso-compositional section were detected. This ternary phase may correspond to the Cu_2TiZr phase observed by Woychik et al. [9].

From the DTA analysis [10], it was determined that by adding Zr to the $CuTi_2$ phase, the liquidus temperature was reduced, reaching a minimum at 36% at. and 839 °C. Beyond that composition, the liquidus temperature was observed to rise again, until it reached the melting point for the stoichiometric composition $CuZr_2$—996 °C. Exothermic effects were observed close to the melting range of the alloys. As will be seen from the calculations presented in this work, these effects could be due to the precipitation of small amounts of other phases, as the section studied was not a perfect quasi-binary system.

3. Thermodynamic models

3.1. Solution phases

The liquid phase was modeled using a single-lattice random solution model. Since all the elements comprising this system form substitutional *fcc*, *hcp* and *bcc* solutions, they can also be modeled using the same single-lattice random solution model. This model takes into account the thermo-chemical interactions between elements present in the lattice and therefore, for all these four phases the Gibbs energy can be expressed as:

$$\begin{aligned} G_m^{\phi} &= \sum_i x_i^{\phi 0} G_i^{\phi} + RT \sum_i x_i^{\phi} \ln(x_i^{\phi}) + {}^{\mathrm{ex}}G_m^{\phi} \\ {}^{\mathrm{ex}}G_m^{\phi} &= \sum_i^{n-1} \sum_{j=i+1}^{n} x_i^{\phi} x_j^{\phi} L_{i,j}^{\phi} \end{aligned} \quad (2)$$

where elements Cu, Ti and Zr are identified as 1, 2, 3; *n* is equal to 3; x_i^{ϕ} is the molar fraction of element *i*; ${}^0G_i^{\phi}$ corresponds to the Gibbs energy of the pure element *i* in the phase; ${}^{\mathrm{ex}}G_m^{\phi}$ is the excess Gibbs energy of the liquid phase; and $L_{i,j}^{\phi}$ is the binary interaction parameter between elements *i* and *j*.

Using the Redlich–Kister formalism [16], the binary interaction parameter $L_{i,j}^{\phi}$ can be further expanded:

$$\begin{aligned} L_{i,j}^{\phi} &= \sum_k {}^k L_{i,j}^{\phi} (x_i^{\phi} - x_j^{L})^k \\ {}^k L_{i,j}^{\phi} &= {}^k a + {}^k bT \end{aligned} \quad (3)$$

As seen in Eq. (3), the binary interaction parameter can also vary with composition and temperature. It is easily recognized that the zeroth order binary interaction parameter corresponds to the regular solution model.

The models describing the thermodynamic behavior of

Table 1
Enthalpies of infinite solution of liquid Cu alloys [3]

Solute	$\Delta\bar{H}$, kJ/mol
Ti	−9.0
Zr	−67.8

the solid solution phases *fcc*, and *hcp* were not re-assessed. The liquid and bcc phases, however, were further modified by adding an extra term to the expression for ${}^{ex}G_m^{\phi}$:

$${}^{ex}G_m^{\phi} = \sum_{i}^{n-1} \sum_{j=i+1}^{n} x_i^{\phi} x_j^{\phi} L_{i,j}^{\phi} + x_i^{\phi} x_{j\neq i\neq k}^{\phi} x_{k\neq i\neq j}^{\phi} L_{i,j,k}^{\phi} \quad (4)$$

where $L_{i,j,k}^{\phi}$ corresponds to the ternary interaction parameter.

The ternary interaction parameter can further be expanded as

$$L_{i,j,k}^{\phi} = \sum_{t=i,j,k} x_t^{\phi} L_t^{\phi} \quad (5)$$

This expansion is particularly useful when the Gibbs energy function for the ternary phase is highly asymmetrical. This usually arises as a consequence of the very different values for the binary interaction parameters of the sub-systems. In the case of the Cu–Ti–Zr system, the Cu–Zr interaction parameter for the liquid phase is twice as negative as the Cu–Ti interaction; reflecting the fact that the enthalpy of mixing of the Cu–Zr system is much more exothermic than that of the Cu–Ti binary (see Table 1), while the Ti–Zr interaction parameter is very small (Fig. 3 shows that Ti and Zr form almost ideal solutions in the liquid and solid phases). Because of the asymmetrical nature of the excess Gibbs energy of the liquid phase for this ternary system, the use of Eq. (5) permits a better modeling of the ternary interaction energies. For a ternary system whose corresponding binary interactions have similar values (the ternary bcc solid solution phase), we can use a single, zeroth-order ternary parameter $L_{i,j,k}^{\phi}$ since $\Sigma_i\, x_i^{\phi} = 1$.

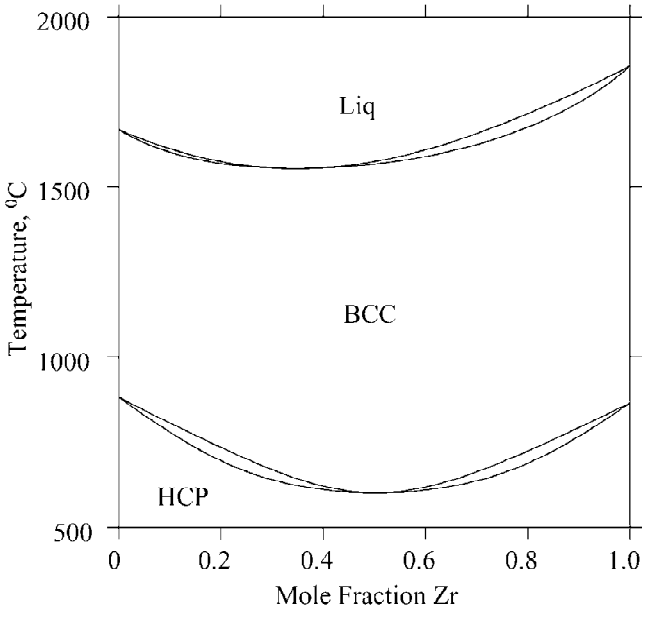

Fig. 3. Calculated Ti–Zr phase diagram, using thermodynamic assessment by Kumar et al. [12].

3.2. Cu_4Ti and CuTi phases

These two phases have relatively wide homogeneity ranges (19.1 to 22 at.% for Cu_4Ti; 48 to 52 at.% for CuTi). Accordingly, Kumar et al. [1] modeled them as if they consisted of ideal end-members Cu_4Ti and CuTi consisting of two sublattices (Cu in one sublattice, Ti in the other) with anti-structure atoms in each of the sublattices. Using the sublattice formalism, these phases are represented as $(Cu, Ti)_p(Ti, Cu)_1$ where $p = 1.4$ for CuTi and Cu_4Ti, respectively. The Gibbs energies for these phases can be represented by

$$\begin{aligned} G_m^{Cu_pTi} = {} & {}^1y_{Cu}\,{}^2y_{Cu}\,{}^0G_{Cu:Cu}^{Cu_pTi} + {}^1y_{Cu}\,{}^2y_{Ti}\,{}^0G_{Cu:Ti}^{Cu_pTi} \\ & + {}^1y_{Ti}\,{}^2y_{Cu}\,{}^0G_{Ti:Cu}^{Cu_pTi} + {}^1y_{Ti}\,{}^2y_{Ti}\,{}^0G_{Ti:Ti}^{Cu_pTi} \\ & + RT\left[p\sum_i {}^1y_i \ln({}^1y_i) + \sum_i {}^2y_i \ln({}^2y_i) \right] \\ & + {}^1y_{Cu}\,{}^1y_{Ti}({}^2y_{Cu} L_{Cu_pTi:Cu,Ti:Cu}^{Cu_pTi} + {}^2y_{Ti} L_{Cu_pTi:Cu,Ti:Ti}^{Cu_pTi}) \\ & + {}^2y_{Cu}\,{}^2y_{Ti}({}^1y_{Cu} L_{Cu:Cu_pTi,Ti}^{Cu_pTi} + {}^1y_{Ti} L_{Ti:Cu_pTi,Ti}^{Cu_pTi}) \end{aligned} \quad (6)$$

In their model, Kumar et al. [1] applied the following constraints:

$$\begin{aligned} {}^0G_{Cu:Cu}^{Cu_pTi} &= (p+1)K \\ {}^0G_{Ti:Ti}^{Cu_pTi} &= (p+1)K \\ {}^0G_{Ti:Cu}^{Cu_pTi} &= {}^0G_{Cu:Cu}^{Cu_pTi} + {}^0G_{Ti:Ti}^{Cu_pTi} - {}^0G_{Cu:Ti}^{Cu_pTi} \end{aligned} \quad (7)$$

where K was defined as an arbitrary parameter with a value of 5000 J/mol. The expressions of the form ${}^0G_{A:B}^{A_aB_b}$ correspond to the Gibbs energies for the compound $(A)_a(B)_b$ and are given by

$${}^0G_{A:B}^{A_aB_b} = \Delta H_f^{A_aB_b} - T\,\Delta S_f^{A_aB_b} + a\,{}^0G_A^{ref} + b\,{}^0G_b^{ref} \quad (8)$$

where $\Delta H_f^{A_aB_b}$ corresponds to the enthalpy of formation of the compound; $\Delta S_f^{A_aB_a}$ represents the entropy of formation; ${}^0G_A^{ref}$ and ${}^0G_B^{ref}$ are the Gibbs energies of the pure components in their standard reference state.

3.3. $CuTi_2$ and $CuZr_2$ phases

In their experimental work on the Cu–Ti–Zr system Chebotnikov and Molokanov [10] determined that the phases $CuTi_2$ and $CuZr_2$ form a continuous series of solid solutions across the entire $x_{Ti} + x_{Zr} = 2/3$ iso-compositional line (see Experimental section). Therefore, it was decided to model the $CuTi_2$ and $CuZr_2$ as a single phase using a two-sublattice model. Cu would occupy the first

sublattice while Ti and Zr atoms formed a random solution within the second sublattice. Accordingly, the sublattice notation for this phase is $(Cu)(Ti, Zr)_2$ and will be identified, from now on, as CuM_2. The Gibbs energy for this phase can be expressed in the following manner:

$$G_m^{CuM_2} = {}^2y_{Ti}\,{}^0G_{Cu:Ti}^{CuM_2} + {}^2y_{Zr}\,{}^0G_{Cu:Zr}^{CuM_2} + 2RT[{}^2y_{Ti}\ln({}^2y_{Ti}) + {}^2y_{Zr}\ln({}^2y_{Zr})] + {}^{ex}G_m^{CuM_2} \quad (9)$$

where ${}^0G_{Cu:Ti}^{CuM_2}$ and ${}^0G_{Cu:Zr}^{CuM_2}$ correspond to the Gibbs energies of the end-members $CuTi_2$ and $CuZr_2$, respectively. The excess Gibbs energy, ${}^{ex}G_m^{CuM_2}$, is expressed as

$${}^{ex}G_m^{CuM_2} = {}^2y_{Ti}\,{}^2y_{Zr}\sum_k {}^kL_{Cu:Ti,Zr}({}^2y_{Ti} - {}^2y_{Zr})^k \quad (10)$$

where ${}^kL_{Cu:Ti,Zr}$ corresponds to the interaction energies between Ti and Zr in the second sublattice while Cu is present in the first sublattice.

3.4. Cu_2TiZr phase

In their study of the isothermal section of the Cu–Ti–Zr system, Woychik and Massalski [9] identified the ternary Cu_2TiZr Laves phase in the central region of the phase diagram. Since no information on its solubility limits is available, it was decided to represent this phase as a stoichiometric compound $(Cu)_2(Ti)_1(Zr)_1$. The Gibbs energy of this compound is given by

$${}^0G_{Cu:Ti:Zr}^{Cu_2TiZr} = \Delta H_f^{Cu_2TiZr} - T\,\Delta S_f^{Cu_2TiZr} + 2\,{}^0G_{Cu}^{ref} + {}^0G_{Ti}^{ref} + {}^0G_{Zr}^{ref} \quad (11)$$

3.5. Binary stoichiometric phases

The rest of the binary intermetallic phases were modeled by [1] and [2] as stoichiometric phases of the form $(A)_a(B)_b$, with Gibbs energies expressed by Eq. (8).

4. Optimization procedure

Since every optimized parameter in the thermodynamic model of a phase has its own physico-chemical meaning, the quality of the optimization is strongly dependent on selection of the adjustable parameters used to describe the phase's Gibbs energy. In theory, the use of a great number of adjustable parameters would lead to complete agreement between the models and all the experimental information available, provided that all the experimental data were consistent with each other. However, instead of being a proper thermodynamic optimization, the process would become increasingly similar to a mere curve-fitting procedure. This approach could lead to serious inconsistencies and unusual extrapolations in regions of the system not accessed through experiments. Therefore, a higher priority is usually given to obtaining a consistent model description for all the phases involved, rather than just adjusting the parameters until a perfect fit to the experimental information is obtained.

For this optimization, the different sets of phases were optimized in different stages. For the CuM_2 phase, a positive zeroth-order interaction parameter was used to allow the phase to become less stable at the central regions of the $CuTi_2$–$CuZr_2$ iso-compositional line. This was consistent with the fact that there is a liquidus depression as the product ${}^2y_{Ti}^2y_{Zr}$ approached a maximum. If it were not for these overall positive interaction energies, the ideal entropic contributions to this phase (see Eq. (9)) would make the phase undesirably more stable in the central region of the $x_{Ti} + x_{Zr} = 0.66667$ line than at the end members. Moreover, a compositional dependency for the $L_{Cu:Ti,Zr}^{CuM_2}$ binary interaction parameter was used to account for observed asymmetries in the solidus as measured by [10].

As has been noted above, the liquid phase presents pronounced asymmetries with regard to the excess Gibbs energy terms corresponding to the assessed binary interactions, with the Cu–Zr interaction being much more negative than those corresponding to the Cu–Ti and Ti–Zr binaries. Due to this fact, it was decided to represent the ternary interaction parameter as shown in Eq. (4). The parameters for the liquid and the solid solution CuM_2 were optimized simultaneously using the liquidus and solidus data provided by [10].

Once the parameters for these two phases were optimized, the invariant reaction data obtained by [9] were used to obtain the Gibbs energies of formation for the ternary phase Cu_2TiZr. In this stage of the optimization procedure, it was found that the invariant reaction $Liq \rightarrow Cu_2TiZr + bcc + CuZr_2$ could not be calculated without compromising the consistency with the rest of the experimental data available. In order to calculate this invariant reaction it was necessary to incorporate a ternary interaction parameter to the thermodynamic description of the *bcc* phase.

After the optimization for the Cu_2TiZr phase was performed, it was observed that the invariant equilibrium reaction involving the phases *Liquid*, $CuTi_2$, CuTi and Cu_2TiZr was not eutectic in character, as was reported by Woychic et al. [9]. Slight modifications to the parameter corresponding to the enthalpy of formation of the Cu_2TiZr phase were made until the reaction in question exhibited the correct character (according to experiments). However, it was found that small modifications to the enthalpy of formation of this phase resulted in relatively noticeable changes in the calculated temperatures for the invariant reactions involving this phase: For example, changing the enthalpy of formation of the Cu_2TiZr phase by just -2 kJ/mol resulted in changes to the invariant reaction temperatures of up to $+30$ °C. Furthermore, the resulting temperatures for at least two of the invariant reactions used in the optimization were above 875 °C, which is higher

than the actual experimental temperatures reported by Woychic et al. [9]. As noted in the experimental section of this work, all the experimentally determined invariant reactions occurred necessarily at temperatures below 865 °C. Calculating the correct temperature range for the invariant reactions used in the optimization was given more statistical weight than obtaining the correct character of the reaction itself (which is by itself difficult to optimize) and therefore the optimized parameters previously obtained were considered as acceptable.

Finally, the parameters obtained for all the phases involved in the experimental data were optimized simultaneously, through several iterations, until a satisfactory agreement between all the data used was achieved. Although the results do not perfectly match the experimental results used for the optimization, the resulting model parameters constitute a consistent representation of the thermodynamic properties of the Cu–Ti–Zr system over the entire compositional range.

5. Optimization results

5.1. Comparison with experimental isothermal sections

Fig. 4 shows the calculated and experimental ternary section for the Cu–Ti–Zr system at 703 °C. The agreement in most of the phase diagram is good, although there are some important discrepancies. First, Woychik et al. [9] have established the existence of a two-phase equilibrium phase field between the phases Cu_3Zr_2 (in more recent studies described as $Cu_{10}Zr_7$) and Cu_3Ti_2. It was found that it was not possible to reproduce this feature of the phase diagram without modifying the descriptions for the Gibbs energies of formation for the binary phases in the Cu–Ti and Cu–Zr systems, as obtained by [1] and [2].

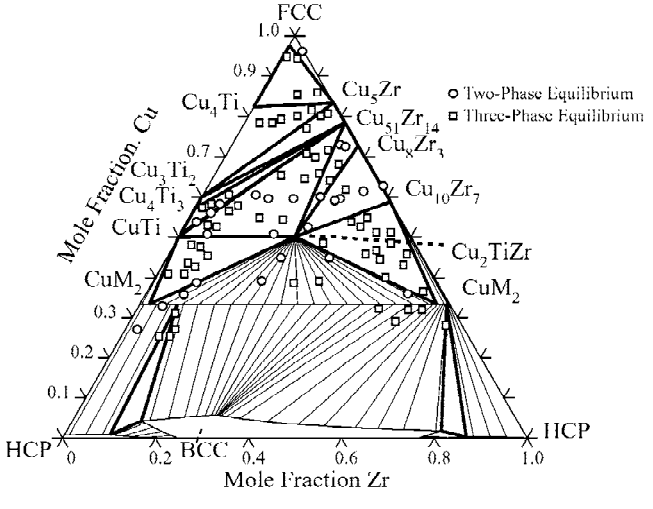

Fig. 4. Calculated vs. experimental ternary isothermal section for the Cu–Ti–Zr system at 703 °C.

This lack of agreement between experiment and calculation could be explained by the relatively low Gibbs energy of formation of the Cu_3Ti_2 compound: according to the thermodynamic descriptions used, the tie-line between the Cu_3Ti_2 and $Cu_{10}Zr_7$ phases becomes metastable with respect to the $Cu_{10}Zr_7$–Cu_8Zr_3–Cu_2TiZr three-phase field. Table 2 shows the calculated Gibbs energies of formation for all the phases close to the $x_{Cu} = 0.6$ iso-compositional line.

In light of these discrepancies, one could be tempted to re-assess the binary systems and modify the values for the Gibbs energies of formation of some (or all) of the binary compounds involved. However, this would in turn generate more discrepancies within the binary systems themselves, since most of the phases involved have rather well established thermodynamic properties. For example, changing the Gibbs energy of formation of the Cu_3Ti_2 phase (making it more negative, so a Cu_3Ti_2–$Cu_{10}Zr_7$ two-phase field is observed) would increase the stability of this phase with respect to the Cu–Ti liquid and CuTi intermetallic compound, changing the phase boundaries and invariant point temperatures involving these phases in the Cu–Ti system. In order to adjust these changes, we would need to modify the descriptions for the Cu–Ti liquid and CuTi intermetallic compound. This would in turn generate discrepancies with well-established values for the thermo-chemical properties of such phases and their relationships with other phases in the system. This cascading effect would spread throughout the thermodynamic descriptions of the Cu–Ti and Cu–Zr systems, implying that probably all the phase descriptions in these systems are incorrect, which is highly unlikely. Therefore, it appears necessary to assess the reliability of the experimental data for the ternary system and the thermodynamic parameters for the binary sub-systems through further studies.

A possible way to test the reliability of the parameters used in the thermodynamic description of the binaries comprising the Cu–Ti–Zr system consists of using them to calculate ternary phase diagrams involving a third element. To this effect, we used the binary description for the Cu–Ti system used in this work; the Cu–Ag description found in [17]; and the Ag–Ti description by [18] to calculate the ternary section at 700 °C of the Ag–Cu–Ti system. Without any ternary interaction parameter incorpo-

Table 2
Calculated Gibbs energies of formation of several phases at 703 °C. Ref. States: fcc and hcp

Phase	ΔG_f J/g-atom
$Cu_{10}Zr_7$	−14220
Cu_8Zr_3	−13460
$Cu_{51}Zr_{14}$	−12975
Cu_2TiZr	−14163
Cu_3Ti_2	−7129
Cu_4Ti_3	−7524

rated to the models—except for a zeroth order interaction parameter for the CuM_2 phase—the calculated ternary phase diagram shows excellent agreement with the experimental data obtained by [19], as shown in Fig. 5. Based on this successful extrapolation of the description for the Cu–Ti sub-system towards another ternary system, we could safely assume that the model parameters describing the Cu–Ti phase relations are reliable enough.

A similar approach for the Cu–Zr system would also be desirable. Through literature search it was found that a model for the Cu–Mg–Zr ternary system—using the same Cu–Zr description [2] that was used in this work—has already been developed by Hämäläinen et al. [20]. In their description, Hämäläinen et al. were able to successfully model the liquidus data of this ternary system over a limited compositional range. Additionally, equilibria between a new ternary phase (Cu_2MgZr) and the $Cu_{51}Zr_{14}$, Cu_8Zr_3 and $Cu_{10}Zr_7$ phases were found to be in good agreement with experimental information. Based on this evidence, the model parameters describing the binary interactions in the Cu–Zr system can be considered to be somewhat reliable, although a more complete analysis of other ternary systems involving this binary sub-system may be needed to establish the overall reliability of the thermodynamic models with greater level of confidence.

If it were then assumed that all the binary compounds have reliable thermodynamic descriptions, the only other explanation for the observed discrepancies between calculated and experimental phase boundaries would be the fact that the $Cu_{10}Zr_7$ phase is non-stoichiometric, as has been observed by [9]. This phase would then have to be modeled with multiple sublattices, allowing for different kinds of point defects in all the sublattices. With the proper parameters, it may be possible to calculate equilibria between this phase and Cu_3Ti_2, without compromising the behavior (and description) of this phase in the Cu–Zr system. However, there are only two data points describing the non-stoichiometry of the phase in question, and we determined that it was not possible to obtain a self-consistent set of parameters for this phase. More information on this area of the phase diagram is needed if a better thermodynamic description is to be obtained.

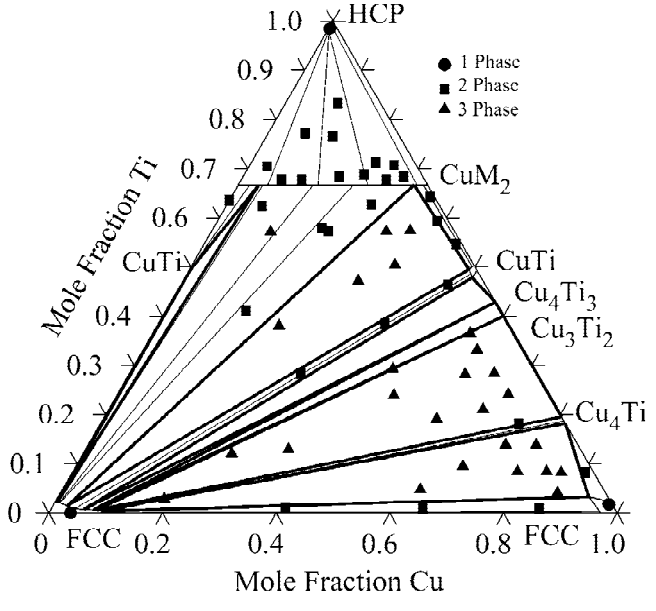

Fig. 5. Experimental and calculated Ag–Cu–Ti Ternary Phase Diagram at 700 °C.

The other important discrepancy is the reported existence of a three-phase field involving the phases *hcp*, $CuZr_2$–$(Cu)_1(Ti, Zr)_2$ with mostly Zr in the second sublattice—and Cu_2TiZr [9]. This contradicts the experiments done by Chebotnikov and Molokanov [10]. As was said above, these authors found that the lattice parameters of the resulting crystalline phases ($CuTi_2$) varied linearly as Zr was interchanged with Ti within the second sublattice of the phase. This linear change through the entire compositional range ($CuTi_2$–$CuZr_2$) could not have been observed if a three-phase field existed across the $x_{Cu} = 0.333$ line, as reported by [9]. Instead of a linear change, the lattice parameter measurements would have produced a plateau in the region where three phases coexisted. Because of the experimental evidence provided by [10], we believe that the three-phase regions Cu_2TiZr-hcp–$CuTi_2$ reported by [9] do not correspond to an equilibrium condition at this particular temperature.

5.2. Comparison with invariant point calculations

One of the most important kinds of experimental data in terms of its usefulness for thermodynamic modeling is the determination of invariant equilibrium points. The consistency between experimental and calculated invariant equilibria constitutes a good indicator of the validity of the thermodynamic descriptions used. As noted above, Woychik and Massalski used the Transient Liquid Phase Bonding (TLPB) technique to determine the existence of invariant points involving the liquid phase and the crystalline phases CuTi, CuZr, $CuZr_2$ and Cu_2TiZr [9]. Table 3 presents a comparison between the calculated and experimental invariant points, including reaction temperatures. One of the most satisfactory results was the successful calculation of the temperatures for the invariant reactions. From TLPB experiments it is not possible to determine the temperatures at which the invariant reaction occurred. However, all the TLPB experiments occurred at

Table 3
Comparison between experimental [9] and calculated invariant points

Ternary Reaction	Temp, °C calc	% at Cu exp/calc	% at. Zr exp/calc
$L \rightarrow CuZr + CuZr_2 + Cu_2TiZr$	833	48.6/44.5	37.5/41.2
$L \rightarrow bcc + CuZr_2 + Cu_2TiZr$	827	39.4/38.5	43.2/29.8
$L + CuTi_2 \rightarrow CuTi + Cu_2TiZr$	856	47.6/44.9	17.8/14.5

temperatures between 855 and 867 °C. In order to observe eutectic (or peritectic) transformations upon quenching of the TLPB diffusion couples, these invariant reactions must have occurred at temperatures below that temperature range. We can see from Table 3 that this is indeed what has been calculated.

From Table 3, it is observed that the calculated compositions for the invariant reactions agree rather well with experiments. The biggest discrepancy between calculations and experiments is the nature of the invariant reaction involving the *Liquid*, CuTi, $CuTi_2$ and Cu_2TiZr phases. Through TLPB experiments, it was determined that this reaction is eutectic in character. In the calculations, however, a peritectic-type reaction is obtained. Fig. 6 shows the calculated surface for primary solidification around the $CuTi_2$–CuTi–Cu_2TiZr–*Liquid* invariant reaction. As can be seen, there exists a eutectic reaction very close in composition and temperature coordinates involving the CuTi–Cu_2TiZr–$Cu_{51}Zr_{14}$–*Liquid* phases. The difference in temperatures between the two reaction points is just 1.3 °C, while the composition for these two reactions is also very close. If the temperature difference between these two invariant equilibria went in the opposite direction, however, the calculated $CuTi_2$–CuTi–Cu_2TiZr–*Liquid* invariant reaction would have been of eutectic type. Although during the optimization it was attempted to obtain the correct type of invariant equilibrium, it was seen that this was not possible without generating more serious discrepancies with other experimental data.

Thanks to the experimental verification of three invariant points involving the Cu_2TiZr phase, it was possible for Woychic et al. to establish the boundaries of the Cu_2TiZr+*Liquid* primary solidification phase field [9]. Since the composition Cu_2TiZr was within these boundaries, it was determined that the compound melted congruently. Calculations using the thermodynamic models just obtained show that the congruent melting temperature of this compound is about 883 °C. This melting temperature is lower than that of any of the surrounding binary compounds.

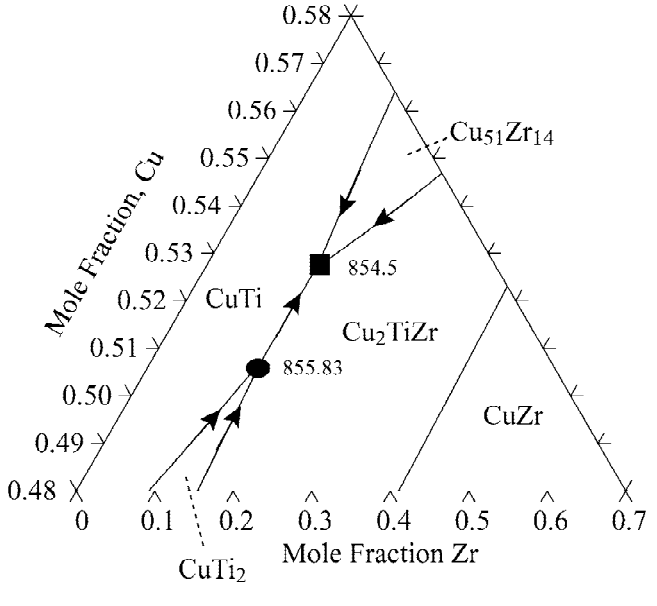

Fig. 6. Calculated primary surface of solidification, temperatures in °C.

In their work on brazing of Ti alloys using Cu–Ti–Zr amorphous metals, Botstein et al. [21] report the use of a 50Cu–25Ti–25Zr amorphous alloy, which corresponds to the composition of the Cu_2TiZr phase. The brazing experiments reported by these authors were performed at 900 °C. Thus, the upper limit to the melting point of the Cu_2TiZr ternary phase would necessarily be around 900 °C. According to our optimization results, this further constraint is satisfied.

Additional verification of the present assessment is the existence of a peritectic reaction involving the Cu_2TiZr and $Cu_{10}Zr_7$ phases. This reaction was observed and reported by Woychik and Massalski [9] from their TLPB experiments at temperatures below 855 °C. Our calculations show that this peritectic reaction occurs at 845 °C.

5.3. Comparison with calculated and experimental pseudo-binary section $CuTi_2$–$CuZr_2$

Fig. 7 shows the calculated and experimental [10] pseudo-binary section $CuTi_2$–$CuZr_2$. As can be seen, very good agreement has been achieved between the points describing the solidus and liquidus lines and the calculated pseudo-phase boundaries. According to the experiments, a minimum in the liquidus temperature is reached in the central region of the phase diagram (33 at.% calculated v.s. 36.7 at.% experimental). At this point, the liquid phase is stable down to 839 °C, which compares well with the calculated value of ~827 °C. It can also be seen that the calculation shows that a continuous series of compositions based on the $(Cu)_1(Ti, Zr)_2$ formula exist at temperatures below 827 °C. The stability of the phase CuM_2 over the entire compositional range from $CuTi_2$ to $CuZr_2$ has been verified experimentally.

In Fig. 7 the different pseudo-phase fields at temperatures below the solidus line indicate the presence of other crystalline phases, such as *bcc* and Cu_2TiZr. It is important to note, however, that the phase fraction of these phases was calculated to be generally below 10^{-9}. The presence of these phases in the calculated pseudo-binary section comes from the fact that it is not a strictly stoichiometric composition. An exception occurs in the central region of the diagram, at temperatures close to that of the minimum in the liquidus. In this region, Cu_2TiZr is present in significant fractions (~0.36). The composition and temperature ranges at which this phase is stable coincide with those indicated by [10], although the ternary phase was not identified in the experiments. In this figure, the invariant reactions $L + CuTi_2 \rightarrow BCC + Cu_2TiZr$ (U9) and $L \rightarrow CuTi_2 + Cu_2TiZr + BCC$ (E5) are also indicated at the middle of the phase diagram. The observed presence of Cu_2TiZr in the experiments by Chevotnikov and

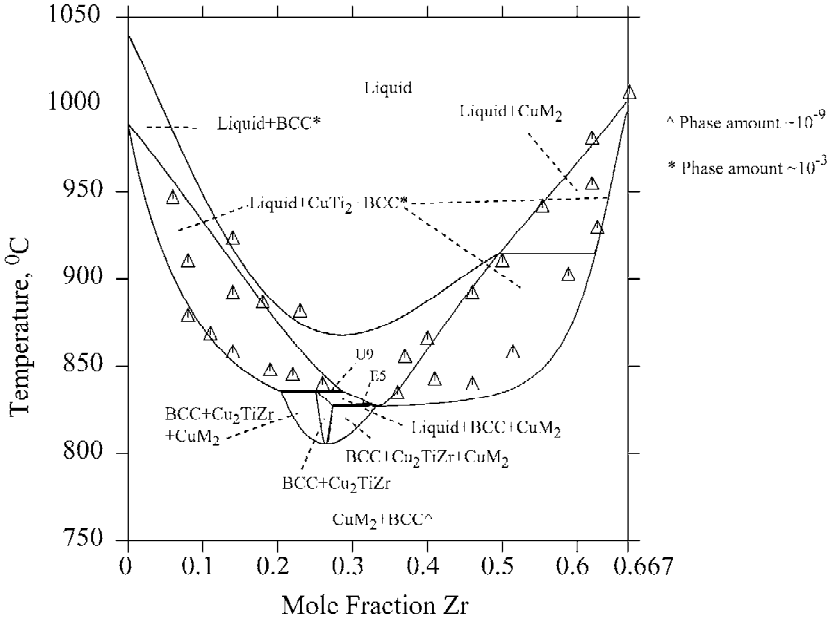

Fig. 7. Pseudo-binary phase diagram $CuTi_2$–$CuZr_2$. Experimental points (△) after [10].

Molokanov [10] could have been the product of either of these two invariant reactions.

Close to the liquidus, the *bcc* phase appears to be present when only the liquid phase is experimentally found. The calculated phase fractions for the *bcc* phase, however, are below 10^{-2}. In what experimentally is the $CuTi_2 + Liquid$ phase field, the *bcc* phase is also present. The phase fraction of bcc in this region is in the order of 10^{-3}. The presence of the *bcc* phase in these phase fields could be an artifice of the numerical thermodynamic calculations using the model parameters obtained in this work. However, even if *bcc* was actually present in the quantities calculated, the experimental detection of this phase would have been very difficult due to its presence in such small amounts.

6. Calculations using the assessed thermodynamic models

From Fig. 8, it can be seen that the liquid phase is stable in two well-defined regions: an elongated area parallel to the Cu–Ti axis of the ternary compositional coordinate system and the central portion of the phase diagram, which is consistent with the liquidus depression observed in the $CuTi_2$–$CuZr_2$ compositional line as reported by Chebotnikov and Molokanov [10]. The elongated region parallel to the Cu–Ti axis coincides with the location of the lowest liquidus line (Cu–Ti binary, $0.2 < x_{Ti} < 0.4$) in any of the binary systems comprising the Cu–Ti–Zr ternary. The liquid phase is stable in the central region of the phase diagram due to two factors represented in the thermodynamic model used for its description: First of all, the binary interaction energies (specially those for the Cu–Ti and Cu–Zr systems) reach a minimum in the central regions where $X_{Cu}/X_{Ti} \approx X_{Cu}/X_{Zr} \approx 1$. Second, the ideal entropy of mixing is maximized at the composition where $X_{Cu} = X_{Ti} = X_{Zr}$.

At temperatures below 883 °C, the ternary phase Cu_2TiZr precipitates and, as temperature decreases, dominates the central portion of the phase diagram, as can be seen in Fig. 11. This ternary phase is expected to play an important role in the amorphisation of alloys in the vicinity of the 0.5Cu–0.25Ti–0.25Zr composition. At 875 °C (Fig. 9) most of the phases present in the binary phase diagrams take part in several equilibria in the Cu–Ti–Zr ternary

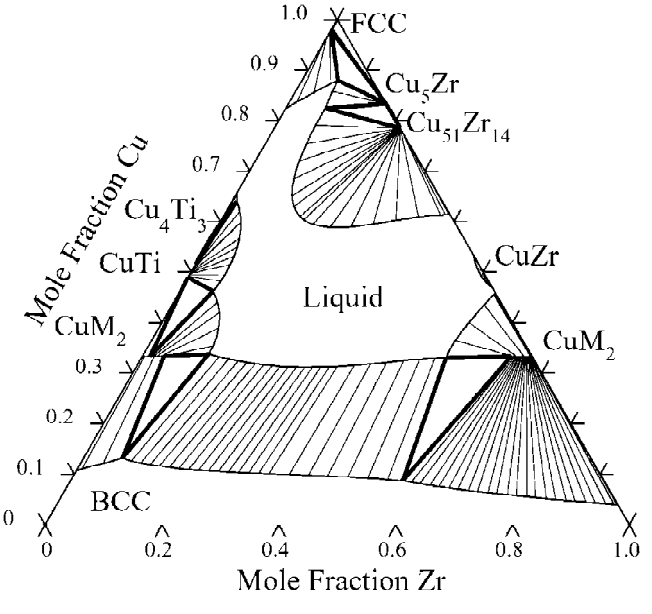

Fig. 8. Cu–Ti–Zr: Calculated isothermal section at 925 °C.

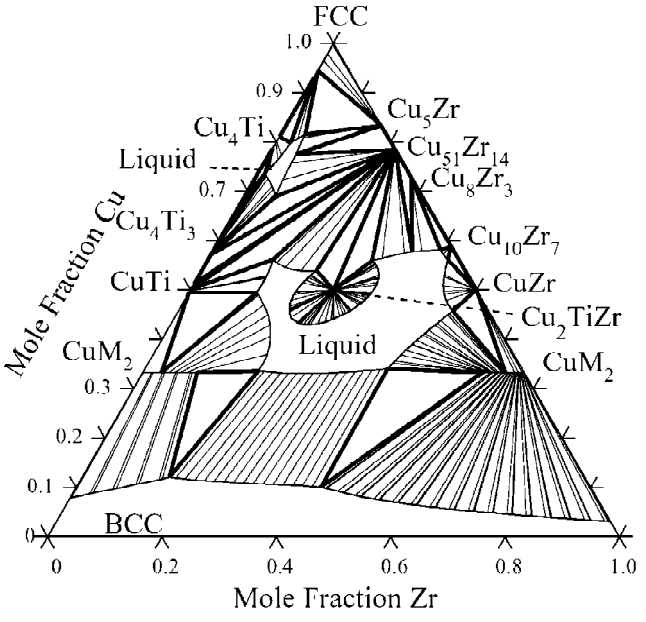

Fig. 9. Cu–Ti–Zr: Calculated isothermal section at 875 °C.

section. Note, from Figs. 4, 8 and 9, that the intermetallic compound CuZr is stable for a limited temperature range (~230 °C), as indicated in Fig. 2.

Fig. 10 shows the calculated liquidus projection for the Cu–Ti–Zr system. The liquidus temperature decreases as the amount of Cu present in the alloy is increased and increases as the Zr corner is approached. It can be seen that at a temperature between 925 and 875 °C, the liquid phase field branches into two topologically non-connected regions. The cusps in the liquidus lines hint at the presence of several ternary invariant points involving the liquid phase. Most of these invariant points also involve the ternary phase Cu_2TiZr.

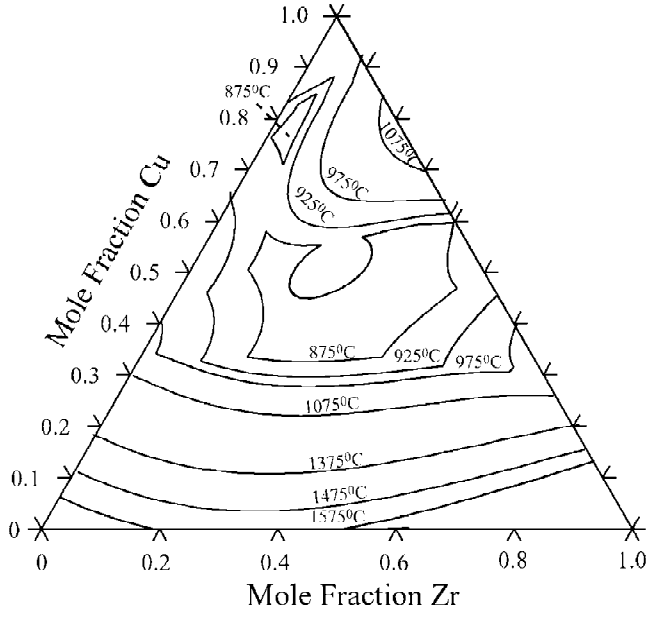

Fig. 10. Calculated liquidus projection for the Cu–Ti–Zr system.

Fig. 11 shows the surface for primary solidification. According to this figure, all the ternary invariant reactions occur at lower temperatures than the neighboring binary invariant points. Thus, throughout the composition range, adding a third element to any given binary sub-system in this ternary increases the stability of the liquid phase relative to neighboring crystalline phases. At Cu-rich compositions, it can be observed that a great number of invariant points involving the $Cu_{51}Zr_{14}$ compound exist. These invariant points are mostly (tributary) peritectic in nature. Fig. 11 shows that of the five eutectic reactions calculated in this system, four involve the Cu_2TiZr phase. These four eutectic points are deep with respect to the temperatures of the neighboring binary invariant reactions. As can be seen in Fig. 11, the lowest liquidus temperatures in the Cu–Ti–Zr system lie along the $x_{Ti} + x_{zr} = 0.667$ iso-compositional line, which is consistent with the data provided by [10]. Moreover, it is interesting to note that the minimum liquidus point in the system seems to lie exactly at the middle of the compositional range, i.e. at the composition $x_{Cu} = x_{Zr} = x_{Ti} = 0.333$. Fig. 12 presents the proposed reaction scheme based on the surface for primary solidification presented in Fig. 11.

7. Summary

The Cu–Ti–Zr system was thermodynamically assessed in order to obtain an optimized and consistent thermodynamic description of all the experimentally-observed stable phases. A new description for the phases $CuTi_2$ and $CuZr_2$ was proposed. The Gibbs energy of formation for the ternary compound Cu_2TiZr was obtained and ternary interactions for the *liquid* and *bcc* phases were assessed. The optimization was performed using the PARROT module of the Thermo-Calc software. It was found that the resulting thermodynamic optimization agreed well with the limited experimental data available, except for some regions of the ternary isothermal section at 703 °C. Isothermal sections and the surface for primary solidification were calculated using the assessed models. It was found that the liquid is more stable at the central region of the phase diagram. More experimental work is needed in order to obtain a more accurate thermodynamic description of the system.

Appendix A

This section contains the parameters used for the assessment of the Cu–Ti–Zr system. Values for ${}^0G_{el}^{\phi}$, where i = Cu, Ti, Zr and $\phi = liq$, *bcc*, *fcc*, *hcp* were obtained from the SGTE database; and are not included in this appendix. Parameters with a '*' have been assessed in this work, otherwise, refer to [1], [2] and [11].

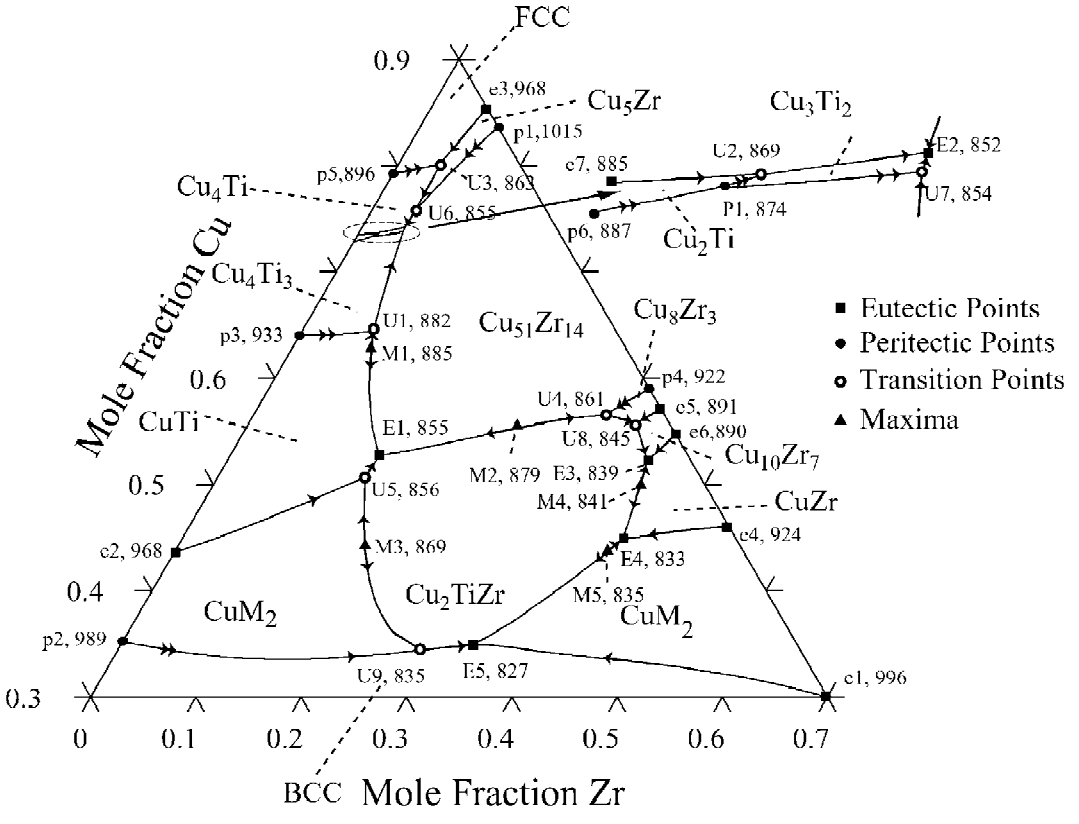

Fig. 11. Surface of primary solidification, temperatures in °C.

Table A.1. Parameters for the liquid phase, J/mol

(Cu, Ti, Zr) Liquid	
${}^{0}L^{\mathrm{Liq}}_{\mathrm{Cu,Ti}}$	$-19{,}330+7.651\cdot T$
${}^{1}L^{\mathrm{Liq}}_{\mathrm{Cu,Ti}}$	0
${}^{2}L^{\mathrm{Liq}}_{\mathrm{Cu,Ti}}$	$+9382-5.448\cdot T$
${}^{0}L^{\mathrm{Liq}}_{\mathrm{Cu,Zr}}$	$-61{,}685.53+11.29235\cdot T$
${}^{1}L^{\mathrm{Liq}}_{\mathrm{Cu,Zr}}$	$-8830.66+5.04565\cdot T$
${}^{0}L^{\mathrm{Liq}}_{\mathrm{Ti,Zr}}$	-968
${}^{\mathrm{Cu}}L^{\mathrm{Liq}}_{\mathrm{Cu,Ti,Zr}}{}^{*}$	$+23{,}828$
${}^{\mathrm{Ti}}L^{\mathrm{Liq}}_{\mathrm{Cu,Ti,Zr}}{}^{*}$	$-28{,}808$
${}^{\mathrm{Zr}}L^{\mathrm{Liq}}_{\mathrm{Cu,Ti,Zr}}{}^{*}$	$+23{,}828$

Table A.2. Parameters for the solid solution phases, J/mol

(Cu, Ti, Zr) BCC	
${}^{0}L^{bcc}_{\mathrm{Cu,Ti}}$	$+3389$
${}^{0}L^{bcc}_{\mathrm{Cu,Zr}}$	-7381.13
${}^{0}L^{bcc}_{\mathrm{Ti,Zr}}$	$-4346+5.489\cdot T$
${}^{0}L^{bcc}_{\mathrm{Cu,Ti,Zr}}{}^{*}$	$-12{,}000$
HCP	
${}^{0}L^{hcp}_{\mathrm{Cu,Ti}}$	$+16{,}334$
${}^{0}L^{hcp}_{\mathrm{Cu,Zr}}$	$+11{,}337$
${}^{0}L^{hcp}_{\mathrm{Ti,Zr}}$	$+5133$
FCC	
${}^{0}L^{fcc}_{\mathrm{Cu,Ti}}$	-9882
${}^{1}L^{fcc}_{\mathrm{Cu,Ti}}$	$+15{,}777$
${}^{0}L^{fcc}_{\mathrm{Cu,Zr}}$	$+2233$

Table A.3. Parameters for CuTi and Cu_4Ti phases, J/mol

$(\mathrm{Cu, Ti})_1(\mathrm{Ti, Cu})_1$	
${}^{0}G^{\mathrm{CuTi}}_{\mathrm{Cu:Ti}}-{}^{0}G^{fcc}_{\mathrm{Cu}}-{}^{0}G^{hcp}_{\mathrm{Ti}}$	$2(-11{,}206+3.272\cdot T)$
${}^{0}L^{\mathrm{CuTi}}_{\mathrm{Cu,Ti:*}}$	$+15{,}419$
${}^{0}L^{\mathrm{CuTi}}_{\mathrm{*:Cu,Ti}}$	$+15{,}578$
$(\mathrm{Cu, Ti})_4(\mathrm{Ti, Cu})_1$	
${}^{0}G^{\mathrm{CuTi}}_{\mathrm{Cu:Ti}}-4\,{}^{0}G^{fcc}_{\mathrm{Cu}}-{}^{0}G^{hcp}_{\mathrm{Ti}}$	$5(-6011+2.339\cdot T)$
${}^{0}L^{\mathrm{CuTi}}_{\mathrm{Cu,Ti:*}}$	$+17{,}089$
${}^{0}L^{\mathrm{CuTi}}_{\mathrm{*:Cu,Ti}}$	$-15{,}767$
Parameters for CuM_2, J/mol	
$(\mathrm{Cu})_1(\mathrm{Ti, Zr})_2$	
${}^{0}G^{\mathrm{CuM_2}}_{\mathrm{Cu:Ti}}-{}^{0}G^{fcc}_{\mathrm{Cu}}-2\,{}^{0}G^{hcp}_{\mathrm{Ti}}$	$3(-12{,}131+4.688\cdot T)$
${}^{0}G^{\mathrm{CuM_2}}_{\mathrm{Cu:Zr}}-{}^{0}G^{fcc}_{\mathrm{Cu}}-2\,{}^{0}G^{hcp}_{\mathrm{Zr}}$	$3(-14{,}634.66+1.730\cdot T)$
${}^{0}L^{\mathrm{CuTi_2}*}_{\mathrm{Cu:Ti,Zr}}$	$+30{,}251$
${}^{1}L^{\mathrm{CuTi_2}*}_{\mathrm{Cu:Ti,Zr}}$	-6200
${}^{2}L^{\mathrm{CuTi_2}*}_{\mathrm{Cu:Ti,Zr}}$	1028
Parameters for Cu_2TiZr, J/mol	
$(\mathrm{Cu})_2(\mathrm{Ti})_1(\mathrm{Zr})_1$	
${}^{0}G^{\mathrm{Cu_2TiZr}}_{\mathrm{Cu:Ti:Zr}}-2\,{}^{0}G^{fcc}_{\mathrm{Cu}}-{}^{0}G^{hcp}_{\mathrm{Ti}}-{}^{0}G^{hcp}_{\mathrm{Zr}}*$	$4(-19{,}094+5.0517\cdot T)$

Table A.4. Parameters for Cu–Ti stoichiometric phases, J/mol

$(\mathrm{Cu})_2(\mathrm{Ti})_1$	
${}^{0}G^{\mathrm{Cu_2Ti}}_{\mathrm{Cu:Ti}}-2\,{}^{0}G^{fcc}_{\mathrm{Cu}}-{}^{0}G^{hcp}_{\mathrm{Ti}}$	$3(-5876)$
$(\mathrm{Cu})_3(\mathrm{Ti})_1$	
${}^{0}G^{\mathrm{Cu_3Ti_2}}_{\mathrm{Cu:Ti}}-3\,{}^{0}G^{fcc}_{\mathrm{Cu}}-2\,{}^{0}G^{hcp}_{\mathrm{Ti}}$	$5(-9249+2.172\cdot T)$
$(\mathrm{Cu})_4(\mathrm{Ti})_3$	
${}^{0}G^{\mathrm{Cu_4Ti_3}}_{\mathrm{Cu:Ti}}-4\,{}^{0}G^{fcc}_{\mathrm{Cu}}-3\,{}^{0}G^{hcp}_{\mathrm{Ti}}$	$7(-9748+2.278\cdot T)$

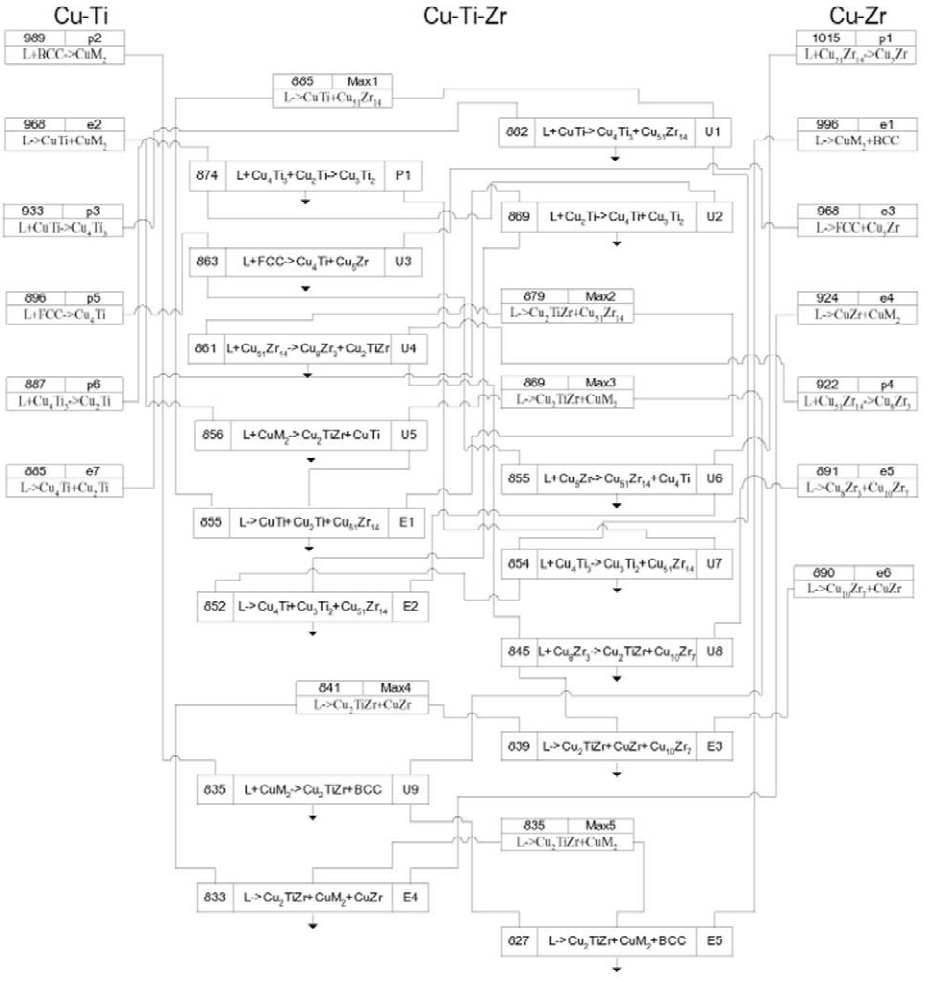

Fig. 12. Reaction diagram for the surface of primary solidification.

Table A.5. Parameters for Cu–Zr stoichiometric phases, J/mol

$(Cu)_5(Zr)_1$ ${}^0G^{Cu_5Zr}_{Cu:Zr} - 5{}^0G^{fcc}_{Cu} - {}^0G^{hcp}_{Zr}$	$6\cdot(-10{,}299)$
$(Cu)_{51}(Zr)_{14}$ ${}^0G^{Cu_{51}Zr_{14}}_{Cu:Zr} - 51{}^0G^{fcc}_{Cu} - 14{}^0G^{hcp}_{Zr}$	$65\cdot(-12{,}975)$
$(Cu)_8(Zr)_3$ ${}^0G^{Cu_8Zr_3}_{Cu:Zr} - 8{}^0G^{fcc}_{Cu} - 3{}^0G^{hcp}_{Zr}$	$11\cdot(-13{,}460)$
$(Cu)_{10}(Zr)_7$ ${}^0G^{Cu_{10}Zr_7}_{Cu:Zr} - 10{}^0G^{fcc}_{Cu} - 7{}^0G^{hcp}_{Zr}$	$17\cdot(-14{,}220)$
$(Cu)_1(Zr)_1$ ${}^0G^{CuZr}_{Cu:Zr} - {}^0G^{fcc}_{Cu} - {}^0G^{hcp}_{Zr}$	$2\cdot(-10{,}052.12 - 3.81598\cdot T)$

References

[1] K.C.H. Kumar, I. Ansara, P. Wollants, L. Delaey, Z. Metallkd. 87 (1996) 666.
[2] K.J. Zeng, M. Hämäläinen, H.L. Lukas, J. Phase Equilibria 15 (1994) 577.
[3] O. Kleppa, S. Watanabe, Met. Trans. B 13B (1982) 391.
[4] N. Saunders, A.P. Miodownik, Mat. Sci. Technol. 4 (1988) 768.
[5] C.G. Woychik, D.H. Lowndes, T.B. Massalski, Acta Metall. 33 (1985) 1861.
[6] A.F. Marshall, Y.S. Lee, D.A. Stevenson, Acta Metall. 31 (1985) 1225.
[7] A. Inoue, W. Zhang, T. Zhang, K. Kurosaka, Acta Mater. 49 (2001) 2645.
[8] X.Y. Yan, Y.A. Chang, Y. Yang, F.Y. Xie, S.L. Chen, F. Zhang, S. Daniel, M.H. He, Intermetallics 9 (2001) 555.
[9] C.G. Woychik, T.B. Massalski, Z. Metallkd. 79 (1988) 149.
[10] V.N. Chebotnikov, V.V. Molokanov, Neorganicheskie Materialy 26 (1990) 960.
[11] N. Saunders, A.P. Miodownik, CALPHAD (Calculation of Phase Diagrams): A Comprehensive Guide, Pergamon Press, Oxford, 1981.
[12] K.C.H. Kumar, P. Wollants, L. Delaey, J. Alloys Comp. 206 (1994) 121.
[13] B. Jansson, Ph.D. Thesis, Division of Physical Metallurgy, Royal Institute of Technology, Stockholm, Sweden, 1984.
[14] B. Sundman, B. Jansson, J.O. Andersson, CALPHAD 2 (1985) 153.
[15] D.S. Duvall, W.A. Owczaeski, D.F. Paulonis, Welding Jnl. 53 (1974) 203.
[16] O. Redlich, A.T. Kister, Ind. Eng. Chem. 40 (1948) 345.

[17] F.H. Hayes, L. Lukas, G. Effenmerg, G. Petzow, Z. Metallkd. 77 (1986) 749.
[18] J.L. Murray, Bull. Alloy Phase Diagrams 4 (1983) 178.
[19] K. Eremenko, Y.I. Buyanov, N.M. Panchenko, Izv. Akad. Nauk SSSR, Metally. 5 (1969) 200.
[20] M. Hämäläinen, N. Bochvar, L.L. Rokhlin, K. Zeng, J. Alloys Comp. 285 (1999) 162.
[21] O. Botstein, A. Schwarzman, A. Rabinkin, Mat. Sci. Eng. A A206 (1996) 14.